Available online at www.sciencedirect.com
ScienceDirect
Journal of Magnetic Resonance 184 (2007) 263–274
JMR Journal of Magnetic Resonance
www.elsevier.com/locate/jmr

SOGGY: Solvent-optimized double gradient spectroscopy for water suppression. A comparison with some existing techniques

Bao D. Nguyen, Xi Meng, Kevin J. Donovan, A.J. Shaka *

Chemistry Department, University of California, Irvine, CA 92697 2025, USA

Received 28 July 2006; revised 27 October 2006
Available online 27 November 2006

Abstract

Excitation sculpting, a general method to suppress unwanted magnetization while controlling the phase of the retained signal [T.L. Hwang, A.J. Shaka, Water suppression that works. Excitation sculpting using arbitrary waveforms and pulsed field gradients, J. Magn. Reson. Ser. A 112 (1995) 275–279] is a highly effective method of water suppression for both biological and small molecule NMR spectroscopy. In excitation sculpting, a double pulsed field gradient spin echo forms the core of the sequence and pairing a low-power soft 180°($-x$) pulse with a high-power 180°(x) all resonances except the water are flipped and retained, while the water peak is attenuated. By replacing the hard 180° pulse in the double echo with a new phase-alternating composite pulse, broadband and adjustable excitation of large bandwidths with simultaneous high water suppression is obtained. This "Solvent-Optimized Gradient–Gradient Spectroscopy" (SOGGY) sequence is a reliable workhorse method for a wide range of practical situations in NMR spectroscopy, optimizing both solute sensitivity and water suppression.

Keywords: Water suppression; Pulsed field gradient; Excitation sculpting; SOGGY; NMR; DPFGSE; WATERGATE; 3-9-19; PURGE; Sucrose; Protein

1. Introduction

The problem of efficient, simple, and robust suppression of strong solvent resonances, in particular the strong water resonance that dominates the spectra of molecules in aqueous solution, has been a focus of attention in the NMR spectroscopy community for many years, and many different methods have been proposed. Some of these methods, such as saturation [1,2] of the H_2O resonance during the relaxation delay that precedes the pulse sequence by a low-intensity continuous irradiation are unsuitable when the solute has protons that exchange with the solvent, as the lines from these exchangeable protons may be attenuated greatly [3] by saturation transfer [4]. The same issues arise in water-eliminated FT (WEFT) pulse sequences [5,6]. Pulsed methods that avoid exciting the water [7–12] avoid the saturation problem, but high suppression can be hard to achieve reliably, and the excitation profile can also result in unwanted attenuation of solute resonances nearby the water, or outside the bandwidth of the excitation.

By far, the most often-used water suppression techniques use pulsed field gradients (PFGs) to rapidly attenuate the H_2O resonance, winding any transverse magnetization into a tight spatial helix oriented along the PFG axis, and causing the integrated magnetic flux through the NMR receiver coil to nearly vanish for the water magnetization. These include gradient-enhanced coherence transfer pathway selection [13], WATERGATE [14], WATERGATE using only hard pulses and delays [15], excitation sculpting [16], WET [17], modifications of WATERGATE [18], and PURGE [19]. All these PFG-based methods have their individual strengths and weaknesses, and may not be applicable in all situations depending on the details of underlying pulse sequence and characteristics of the sample itself. In some cases, the water suppression performance can vary, or be apparently erratic using the same sequence

* Corresponding author. Fax: +1 949 824 9920.
E-mail address: ajshaka@uci.edu (A.J. Shaka).

1090-7807/$ - see front matter © 2007 Published by Elsevier Inc.
doi:10.1016/j.jmr.2006.10.014

on different samples. This may necessitate somewhat tedious trial-and-error optimization of the water suppression to get usable spectra, and is worthwhile avoiding if possible.

By analyzing the PFG-based schemes using a simple theory, and exploring the possible factors that influence performance, we arrive at an improved water suppression sequence based on the previous excitation-sculpting [16] template. This solvent-optimized double gradient spectroscopy (SOGGY) sequence seems to be a good compromise between convenience and performance in many practical situations.

2. Theory

In 1995, Hwang and Shaka [16] outlined a general and flexible way to suppress the strong water resonance using a double pulsed field gradient spin echo (DPFGSE) sequence: G_1-S-G_1-G_2-S-G_2. Here S denotes an arbitrary sequence of radiofrequency (RF) pulses and G_i are mathematically independent PFGs. The analysis, focused on a single uncoupled resonance line and neglecting any dynamics that may arise from the presence of the spatial magnetization helix itself or radiation damping (see below), concluded that the double echo is a *filter* that, for any arbitrary sequence of pulses S, attenuates all transverse magnetization by P^2, the *square* of the "spin flip probability" P,

$$P = \frac{1}{2}\left(1 - \frac{M_z}{M_0}\right). \tag{1}$$

Starting with equilibrium z-magnetization M_0 and calculating the inversion performance of the sequence S gives the z-magnetization, M_z, after S is applied. Eq. (1) ties zero inversion ($M_z = M_0$) with zero spin flip probability, and complete inversion ($M_z = -M_0$) with unit spin flip probability; P is all that is necessary to assess the theoretical double echo performance. All transverse magnetization is attenuated in amplitude by P^2, and has the same phase as before the double echo filter [16] (neglecting homonuclear coupling). It does not matter that S is *not*, in fact, applied to z-magnetization in the experiment itself. Eq. (1) is just a simple and convenient way to compute the number P, which is a function of normalized resonance offset, $\Delta B/B_1^0$, nominal radiofrequency (RF) pulse amplitude, B_1/B_1^0, and any details of the sequence S itself, i.e.,

$$P \equiv P(\Delta B/B_1^0, B_1/B_1^0, S). \tag{2}$$

As P can be engineered, by the choice of S, to attenuate or "chip away" magnetization, but cannot increase magnetization, the term *excitation sculpting* [16,20] was coined for the DPFGSE method. We may consider the total sample magnetization available after a 90° read pulse in the same way a sculptor contemplates a featureless block of marble: choosing the correct sequence of pulses S discards unwanted magnetization and reveals whatever underlying profile is dictated by Eq. (1). Under any DPFGSE we have

$$M_x \to P^2 M_x; M_y \to P^2 M_y; M_z \to (1-2P)^2 M_z. \tag{3}$$

In deriving Eq. (3) it is assumed that the gradients G_1 and G_2 of the DPFGSE are (i) independent and (ii) essentially infinite, so that no complex refocusing of magnetization occurs. While "independent" would follow without question if the spatial axes of the gradients were different, the theoretical performance is also obtained using only z-axis PFGs, by varying the intensity and/or duration of each PFG to avoid any accidental refocusing of magnetization.

This simplified theory, which treats all spins as spatially fixed, isolated, non-interacting, and neglects relaxation or exchange during the double echo, is known to be less than adequate in some situations. For example, it is known that modest gradients in conjunction with high-field magnets, where radiation damping [21,22] can be an issue, can cause some "chaotic" refocusing of magnetization to be observed [23]. Such "resurrection of crushed magnetization" could manifest itself as poor suppression, especially in small-molecule applications where the narrow resonance lines demand longer acquisition times for optimum sensitivity and resolution. As such, water suppression in protein NMR may, in some cases, be less onerous than in small-molecule NMR. The shorter acquisition time of 50–100 ms that is usual and sufficient to digitize wide protein peaks may terminate before the nonlinear feedback that gives rise to unwanted water magnetization has a chance to resurrect the H_2O signal. The water signal then may reappear but not actually be recorded, giving the illusion of good solvent suppression—an illusion as good as reality as far as the protein spectra are concerned. General-purpose water suppression should therefore be measured with quite long acquisition times, just to make sure that the water *stays* suppressed.

The so-called "flip-back" techniques [3] that are employed to optimize the sensitivity of exchangeable protons, typically NH amide protons in proteins, may also improve the suppression by either minimizing the transverse water magnetization at the beginning of the filter, or by suppressing renegade chaotic refocusing of magnetization, or both. For small molecule applications there is no need to try to keep the strong water magnetization along the z-axis, so there is more flexibility in choosing the sequence. Whatever the particular conditions may be, the important characteristics of the solvent suppression sequence are that the strong solvent line(s) are sufficiently attenuated that the dynamic range of the receiver is not an issue, that the spectral baseline is flat, that the sequence is easy to set up and use, that the results are reproducible, and that the desired solute signals are not attenuated too much, so that best sensitivity is obtained.

2.1. Soft-pulse single and double echoes

One point to clear up is that single and double PFGSE sequences with similar notch bandwidth require essentially the same time to complete. This is shown schematically in

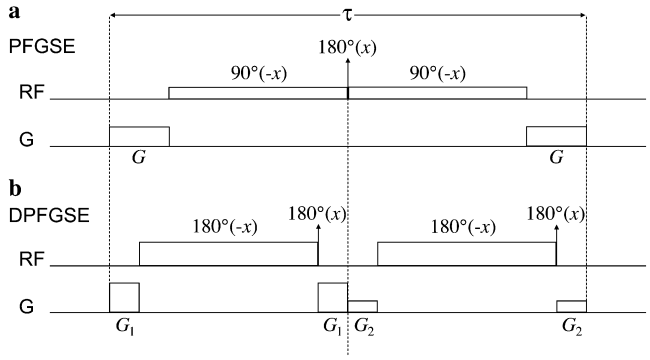

Fig. 1. (a) A pulsed field gradient spin echo (PFGSE) using soft 90° pulses and a strong 180° pulse to flip all spins except those within the bandwidth of the soft pulse. For WATERGATE, the transmitter offset is set right at the H_2O resonance and the notch bandwidth is simply related to the length of the soft pulses. (b) A double PFGSE in which the two soft pulses are now 180° pulses of the same duration, and twice the amplitude as the soft 90° pulses in (a).

Fig. 1. It is crucial to realize that the double echo sequence is *not* a double WATERGATE sequence in terms of duration, a situation that has caused some confusion in the literature [18]. The double and single echo sequences also perform similarly for similar duration, as shown by the calculated attenuation profiles in Fig. 2. Both profiles are broadly similar, the PFGSE showing a slightly wider notch, and the DPFGSE showing a slightly bigger first sidelobe. If this were the whole story, there would be little point in coding the more complex DPFGSE compared with the PFGSE.

The spin–flip probability argument also pertains to the WATERGATE sequence [14,15], in which case the suppression ratio is P rather than P^2. The magnetization phase in WATERGATE, or any single-echo sequence, carries a phase factor φ that depends on the details of the sequence, and that is constant when the echo sequence has perfect symmetry within the PFGSE; departure from symmetry can lead to an unwanted frequency-dependent phase that may be nonlinear. In addition, when *any* kind of error or non-ideality increases P from the ideal value of zero around the water frequency, the DPFGSE with its P^2 dependence will deliver much higher water suppression than WATERGATE.

An example of a nettlesome imperfection is the relative phase between the soft and hard pulses in the echo sequences. For typical conditions, a 2 ms soft 90° pulse and 20 μs hard 180° pulse might be used, giving a dynamic range exceeding 45 dB. Attenuators show some mild phase-dependence over such large changes in amplitude, and a few degrees change in absolute RF phase over this kind of range would be a reasonably good specification. However, such a slight departure from perfect phase degrades the suppression of soft-pulse WATERGATE substantially, as shown in Fig. 3. The pulses are all correctly calibrated, spatially homogeneous, and the calculation of P is done at exact resonance, the water frequency. A phase deviation of as little as 5° brings the theoretical water suppression

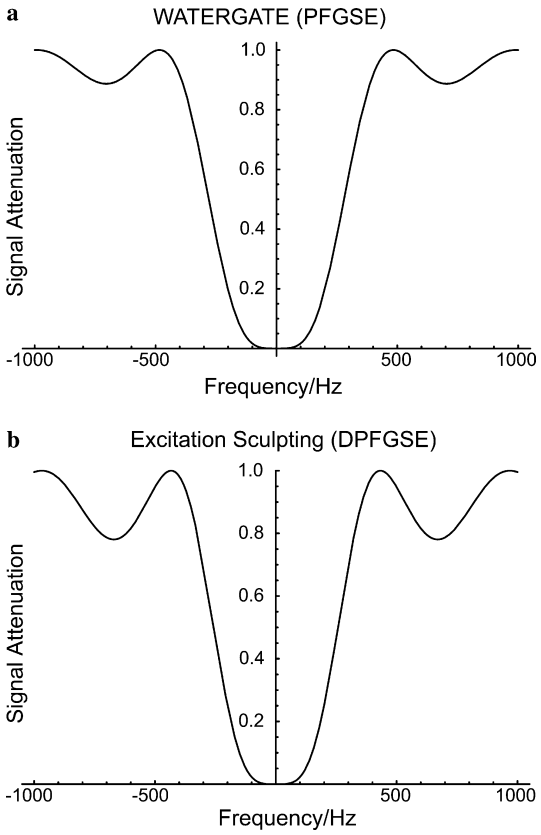

Fig. 2. The theoretical suppression achieved by the sequences of Fig. 1, using 2 ms soft rectangular pulses and assuming ideal pulse calibration, δ-pulses for the hard pulses, and perfect PFGs. (a) WATERGATE profile as a function of frequency. The first maximum is at 484 Hz. (b) Excitation sculpting profile as a function of frequency. The first maximum is at 433 Hz, but the loss of signal at the first lobe is slightly larger than with WATERGATE, a result of the P^2 dependence of the attenuation. In both sequences, using shaped soft pulses can reduce the sidelobe attenuation, at the cost of increasing the width of the notch.

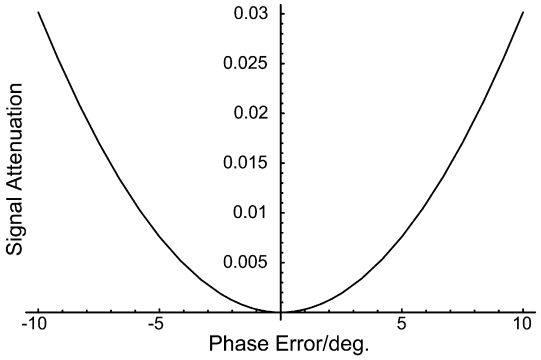

Fig. 3. Predicted performance of WATERGATE as a function of the deviation φ of the soft 90° pulses from their correct setting. The pulses are all assumed to be perfect except for the phase error. The spin flip probability is just $\sin^2\varphi$. This function rapidly gives unacceptable suppression ratios when φ exceeds a few degrees.

down from infinity to a factor of only 132. Experimentally, the phase of the soft pulse may be optimized in small steps to get best performance. But each time the length, and hence power, of the soft pulse is altered, the phase shift

may change slightly, giving the appearance of erratic water suppression and necessitating repetitive optimization. We have verified the sensitivity to small phase errors shown in Fig. 3 by some simple experiments (data not shown). Not surprisingly, an alternative implementation of WATERGATE, using only hard pulses and delays, was adopted quickly by the biomolecular NMR community. By avoiding any change in power, phase errors were also avoided. Note that the excitation sculpting sequence of Fig. 1 shows *no* degradation of performance with respect to such a phase error under the conditions that pertain to Fig. 3. Only when both spatial inhomogeneity and phase error are simultaneously present is there any predicted degradation of performance, and the degradation is insignificant: a 10° phase error and simultaneous 20% departure from nominal B_1 (i.e., 144°($-x$) 144°(x)) still gives $>10^6$-fold theoretical water suppression at exact resonance.

2.2. 3-9-19 Watergate

As noted above, by avoiding soft pulses altogether, the slight phase shifts of such attenuated pulses are also avoided, and this can be done by utilizing hard pulses and delays to flip the off-resonance spins while suppressing the water. By symmetry, only 180° phase shifts are required, and the task is simply to optimize the profile to invert the solute lines but not the solvent line, without using too many pulses. This exercise led to the popular 3-9-19 WATERGATE implementation [15] in which the soft 90°($-x$), hard 180°(x), soft 90°($-x$) refocusing element is replaced with the following:

$$3\alpha(x) - \tau - 9\alpha(x) - \tau - 19\alpha(x) - \tau - 19\alpha(-x) - \tau - 9\alpha(-x) - \tau - 3\alpha(-x) \quad (4)$$

with $26\alpha = 180°$. The sequence of Eq. (4) is applied on resonance with the water, but can be adapted for off resonance application as well [15]. This workhorse sequence gives excellent results but does have one drawback, namely that there is but one adjustable parameter, the delay τ, and this must be optimized to give best sensitivity for solute signals, making the width of the notch around the water of fixed width. The sequence shows a periodic probability profile with respect to frequency: if the pulses are approximated by δ-pulses then there are an endless series of notches at frequencies of $\pm n/\tau$, just as in any DANTE [24] sequence. Fig. 4(a) shows the calculated profile obtained with the 3-9-19 sequence, of 2 ms length ($\tau = 400$ μs). The sequence is not as absolutely flat near the origin as the soft-pulse sequences, but the width of the notch is quite narrow. The performance suffers at offsets approaching the $1/\tau$ condition, as shown in Fig. 4(b), though in protein NMR this condition can be set outside the usual range of amide resonances [15]. But the periodicity precludes using a longer 800 μs delay, to give a sequence of the same length as those of Fig. 2. There is also less of a dropout at frequencies where the soft-pulse sequences show sidelobes due to the rectangular soft pulses; using a shaped soft pulse instead of a rectangular soft pulse gives similar performance to 3-9-19. For resonances beyond 11 ppm, the unavoidable additional notch due to the periodicity of the profile becomes a disadvantage. If signals within 1 ppm of the H_2O line and well beyond 11 ppm are present, it just may not be possible to obtain optimum sensitivity with this sequence even at high field, whereas with the soft-pulse versions this is not an issue.

2.3. Optimizing strong pulse performance

While the delay τ in the 3-9-19 WATERGATE sequence is the primary factor limiting the passband, at large enough offsets the finite pulse width of the hard pulses themselves will reduce the signal. Nonzero hard pulse width also affects the soft-pulse water suppression sequences shown in Fig. 1. In soft-pulse WATERGATE the conventional hard 180° pulse has a finite bandwidth, and so some

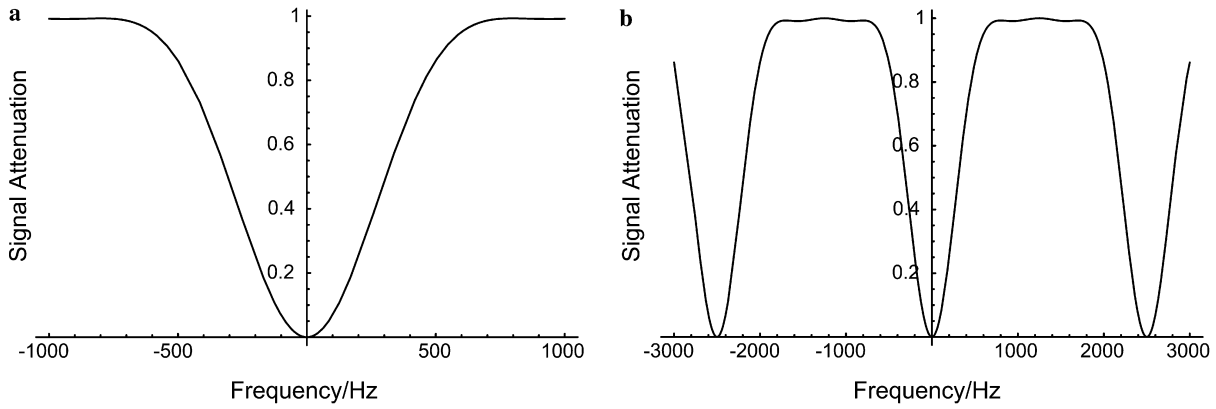

Fig. 4. Predicted performance of 3-9-19 WATERGATE assuming δ-pulses and with a delay $\tau = 400$ μs (*ca.* 2 ms for the entire sequence). (a) The suppression around exact resonance is not quite as flat as with the soft-pulse version, but the notch is quite narrow, with only 20% signal loss at ±1 ppm from the water. (b) The passband shows good flatness, too. The periodic nature of the profile causes another pair of notches at ±2.5 kHz, which would be around 5 ppm away from the water resonance at 500 MHz. Extending the performance past 11 ppm downfield necessitates a substantially shorter interpulse delay, of around 300 μs which would result in 20% signal loss at ±1.3 ppm from the water.

attenuation at larger resonance offsets could occur. This loss of signal is exacerbated in excitation sculpting, as two 180° pulses have to be used, and only spins flipped by *both* inversion pulses contribute to the final signal. If the 180° pulse is incorrectly calibrated, or if the RF field is somewhat inhomogeneous over the sample volume, further loss of solute signals will occur.

Fig. 5 shows the expected loss of signal amplitude for the sequences of Fig. 1, as a contour plot versus normalized resonance offset ($\Delta B/B_1^0$) and RF inhomogeneity (B_1/B_1^0). At offsets of 25% of $\gamma B_1^0/2\pi$ the expected loss is around 6% and 12% for the single and double echo sequences, respectively, even if the pulses are perfectly calibrated. If a 10 μs 90° pulse width can be achieved, which is usually possible, the losses are less than these percentages over a ±6 kHz bandwidth from the water resonance, which would be a generous ±12 ppm proton range at 500 MHz. Note, however, that the compensation for B_1 homogeneity is poorer off-resonance.

Excitation sculpting offers considerable flexibility in designing a soft-pulse 180°($-x$), hard-pulse 180°(x) combination. As there is no problem with slight phase errors with excitation sculpting, and there are no unwanted notches in the excitation profile, optimizing the hard pulse to achieve the requisite excitation bandwidth, while reserving the length of the soft pulse to independently adjust the width of the notch at the water frequency, is an attractive proposition for general-purpose water suppression. There are plenty of broadband composite 180° pulses that could be tried. For example, a broadband inversion pulse (BIP) [25] that will flip all the solute spins and that is compensated for inhomogeneity could be substituted for the conventional 180° pulse that was originally suggested by Hwang and Shaka [16]. Unfortunately, the spatial inhomogeneity of the soft 180°($-x$) pulse needs to be accurately refocused by the hard pulse: a BIP gives close to perfect inversion, and this does not match the imperfect performance of the soft pulse. The result is that while very good solute intensity is obtained, the water suppression suffers. We confirmed this disappointing prediction by experiment (data not shown).

To develop the SOGGY sequence, we thus searched for an alternative composite 180°(x) pulse to pair with the soft 180°($-x$) pulse, keeping the following points in mind: (i) the performance of the composite pulse should, on resonance, mimic that of a conventional hard 180°(x) pulse with respect to RF inhomogeneity; (ii) the overall duration of the composite pulse should not add appreciably to the total sequence; (iii) the inversion off resonance should be compensated for RF inhomogeneity, and flat over a considerable frequency bandwidth, to optimize the sensitivity of the solute signals; and (iv) the composite pulse should consist of multiples of some basic length, for simple implementation.

Point (i) is handled by using a phase-alternating composite pulse [26] with a net flip angle of exactly 180°. On resonance, any sequence of x and $-x$ pulses commute regardless of the flip angles, so that making the net flip angle 180° will exactly compensate the spatial inhomogeneity of the soft rectangular pulse, or any kind of amplitude modulated soft pulse. Point (ii) is not an issue, as the offset range that has to be covered is only out to $\pm\gamma B_1/2\pi$ at most, and composite pulses with good performance over this range are not inordinately long. Point (iii) is trickier because the pulse should show excellent compensation for RF inhomogeneity, but *only* off resonance. This means that the effective field B_{eff} should be tilted somewhat over the solute passband, because only by using pulses that do *not*

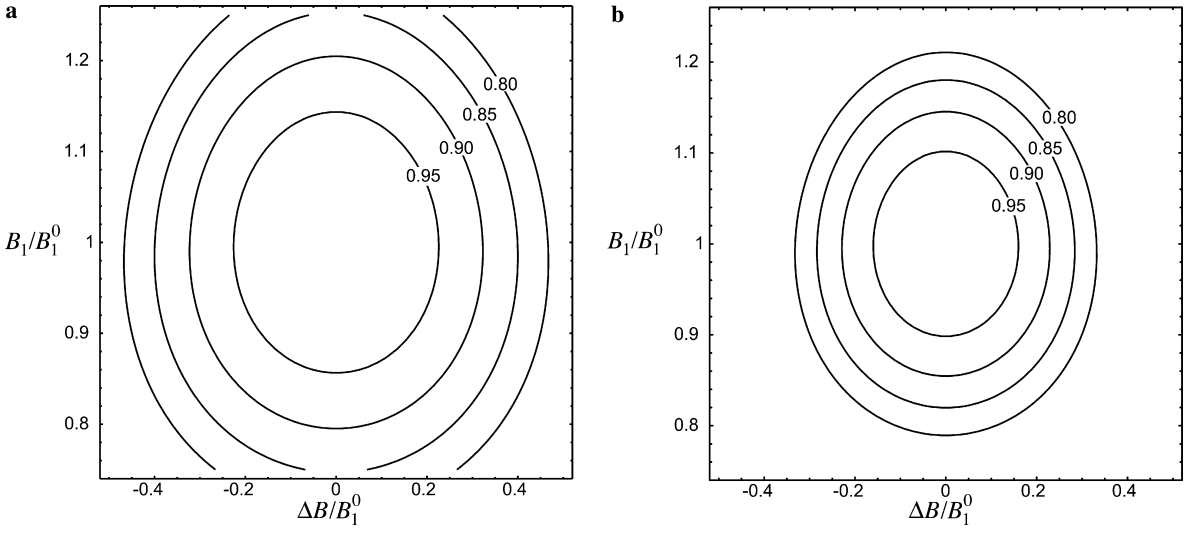

Fig. 5. Spin flip probability profiles for a conventional 180° pulse, plotted versus the dimensionless resonance offset parameter $\Delta B/B_1^0$ and dimensionless RF amplitued B_1/B_1^0. (a) Spin flip probability P. This map is relevant for soft-pulse WATERGATE [14] using a conventional 180° hard pulse. (b) Spin flip probability squared, P^2. This map applies to the DPFGSE sequence of Hwang and Shaka [16]. Miscalibration of the hard 180° pulse can result in significant loss of sensitivity. The DPFGSE sequence also requires a shorter pulse width to excite the usual proton bandwidth. For salty samples, where short pulses can be hard to achieve, the restricted resonance offset range could be a drawback.

commute can any compensation for RF inhomogeneity be obtained. On the other hand, the RF field B_1 should not be too low for the "hard" pulses or the overall duration of the composite pulse will creep up. For operation at 500 MHz we settled on a compromise of a 40 μs 90° pulse width ($\gamma B_1/2\pi = 6.25$ kHz), so that several ppm from the H_2O peak the B_1 field will be somewhat tilted, and some compensation can be achieved with the right choice of composite pulse. A composite pulse of several hundred microseconds results, but for most applications this increase was deemed acceptable compared with the necessary duration of the soft pulses and PFGs. Point (iv) is addressed by noting that a 9° pulse is 4 μs, so that making all pulses a multiple of 9° ensures simple implementation that will not tax even older waveform generation hardware. As a potential side benefit, a 40 μs hard ^{1}H 90° pulse width is possible to achieve on almost any kind of sample, even with considerable salt present. This could be useful with older, less salt-tolerant probes, where tuning and matching capacitors may not have sufficient range to adjust to salty solutions. At higher magnetic field strengths the pulses can be inversely scaled to shorter widths, with a generous 20 μs ^{1}H 90° pulse width being all that is required to run SOGGY at 1 GHz.

Fig. 6 chronicles the line of thought that led to the SOGGY composite pulse. The 90°(x) 180°($-x$) 270°(x) or "123"

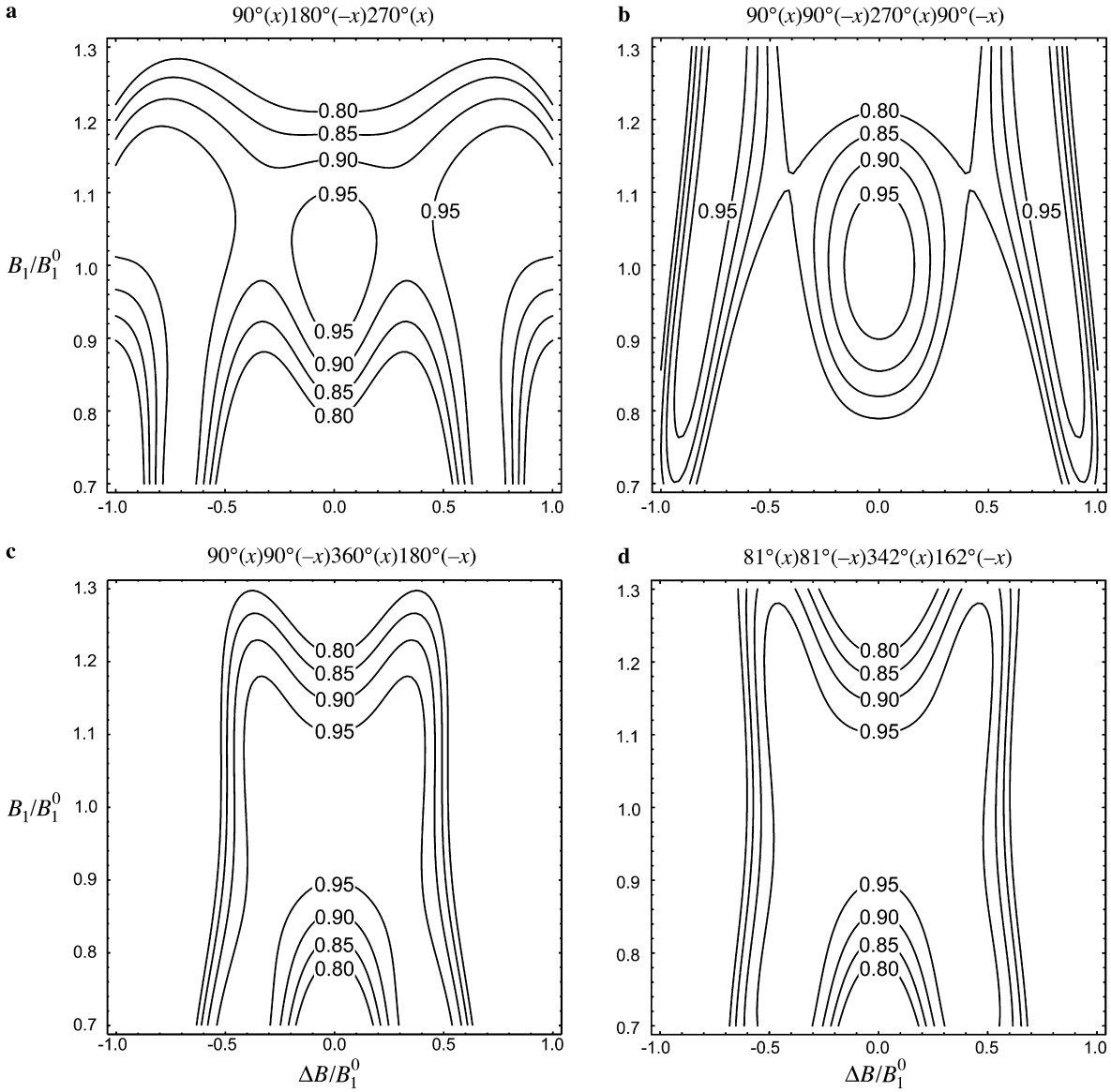

Fig. 6. Contour plots of the square of the spin flip probability, P^2, versus $\Delta B/B_1^0$ and B_1/B_1^0 for some phase-alternating composite 180° pulses. (a) The WALTZ composite pulse shows some broad shoulders of better signal retention, but the intervening offsets are not as good as the response from a conventional 180° pulse (Fig. 5(b)). (b) Permuting a 90° pulse to the rear of the sequence gives this map, in which two "streaks" of good B_1-compensation show up at large resonance offsets. (c) Increasing the flip angles of the last two pulses contracts the region of compensation in toward resonance, so that a much improved profile results. (d) Minor optimization of the sequence in (c) gives the SOGGY composite pulse. The composite pulse has symmetry with respect to offset performance, and so can be executed with the pulses as written, or in reverse order.

inversion pulse used in WALTZ-16 [27,28] gives the spin–flip probability profile shown in Fig. 6(a). Performance off resonance is of interest here, and it is clear that it is possible to compensate the inversion performance for changes in B_1 far off resonance ($\Delta B = 0.75B_1^0$) without changing the on-resonance dependence. However, the profile of Fig. 6(a) is far from ideal as the compensation over the intermediate region, and the compensation for stronger than nominal fields is not good. Also, the region of compensation is too far off resonance, corresponding to *ca.* +14 or −4.5 ppm using a 40 μs 90° pulse width. By removing a 90° segment from the second pulse and reintroducing it at the end of the sequence, yielding 90°(x) 90°($-x$) 270°(x) 90°($-x$), the probability profile of Fig. 6(b) emerges. This profile is worse than 6(a) except with respect to the excellent and more symmetrical B_1 compensation very far off resonance ($\Delta B = \pm 0.95B_1^0$). By gradually increasing the flip angles of the final two pulses, from 270°(x) 90°($-x$) to 360°(x) 180°($-x$), giving 90°(x) 90°($-x$) 360°(x) 180°($-x$) the much-improved "butterfly" profile of Fig. 6(c) results. This profile is clearly much better than its predecessors. At all resonance offsets over the operating bandwidth, the B_1 compensation is better than on resonance and the sweet spot is drawn in to ($\Delta B =$ 0.20 to $0.4B_1^0$) or 7.3 to 9.8 ppm downfield for a 40 μs 90° pulse width. Finally, minor optimization leads to the SOGGY inversion element, 81°(x) 81°($-x$) 342°(x) 162°($-x$), in which the butterfly spreads its wings slightly, giving the nearly ideal spin–flip profile shown in Fig. 6(d). There are, of course, many related phase-alternating sequences that could be used. They differ mostly in detail, and the simplicity and brevity of the four-pulse SOGGY sequence led us to prefer it to more elaborate sequences with 6, 8 or 10 individual pulses, which we have identified by a simple and exhaustive computer grid search. The SOGGY composite inversion pulse can conveniently be implemented as the four-pulse sequence 36 μs (x) 36 μs ($-x$) 152 μs (x) 72 μs ($-x$) assuming a 40 μs 90° pulse width. The simulations assume zero delays between the pulses, a simplification we could relax easily. Most modern spectrometers can shift phase within a few microseconds, and there is no significant degradation of the performance in this case.

3. Experimental

Water suppression would certainly be simpler if it were done strictly within the digital confines of computer simulation. However it is, of course, carried out in the lab using imperfect software and hardware, and sometimes in environments that are less than perfect. All practical matters related to spectrometer performance, unexpected effects from intense lines at high fields, and the balance between convenience and robustness on one hand, and absolute performance on the other, are best settled by careful, controlled experiments. We focus exclusively on water suppression in what follows, although any single strong solvent line can be suppressed in much the same way. The case of multiple solvent lines falls outside the scope of our experiments here.

All the experiments were performed at 500 MHz and executed on a Varian UnityPlus spectrometer console using a conventional H{CN} triple resonance probe with triaxial pulsed field gradients. Only z-PFGs were used in the experiments. The console itself is now far from state of the art, so that the performance shown could probably be improved on a more modern console with better RF performance. As mentioned above, short acquisition times can inadvertently mask poor water suppression. As such, we always acquired FIDs that were long enough that no new signals could possibly contribute at later times. These FIDs were then apodized slightly, to avoid including large amounts of noise from the long tail of the acquisition time. The gentle apodization function did not affect the degree of suppression in any of the experiments.

The practical water suppression results we obtained were stable and reproducible. The spectra shown are representative, and not statistical outliers or best-case results. The new SOGGY sequence was particularly reliable, and delivered high water suppression time after time.

4. Results and discussion

4.1. Radiation damping and anomalous refocusing

Methods that manipulate z-magnetization, such as WET [17] seem anecdotally to require extensive optimization for best performance. Such optimization is partly necessitated by having a number of adjustable parameters. But there is also another difficulty when working with repetitive sequences of the type α_i–G_i (exciting transverse magnetization and then winding it into a tight helix with a gradient) as in WET. The potential problem has been elegantly elucidated by Lin et al. [23]. Calculations and experiments show that the spatial magnetization helix developed by the gradient becomes unstable under some conditions, especially for strong lines that show radiation damping and gradients that not sufficiently strong [23]. Fig. 7 shows the result we observed using a 90°(x)–G–Acquire pulse sequence on a 90% H_2O sample at 500 MHz. While the FID is initially of negligible amplitude, a spontaneous echo-like signal forms at later times; it would transform to a rapidly oscillating residual line shape in a phase-sensitive spectrum. These kinds of residual solvent line shapes are often observed, in a variety of experiments.

To compensate for T_1 relaxation during a repetitive α_i–G_i–τ_i sequence, some flip angles α_i may be set to values larger than 90° [17]. At high field, radiation damping of inverted water magnetization is significant and unexpected effects can occur [22]. Fig. 8 shows the FID that results from a 180°(x)–G–Acquire pulse sequence on a 90% H_2O sample at 500 MHz, using a very large gradient G. Once again, the water signal reemerges and becomes very large. We have observed this behavior no matter how strong the

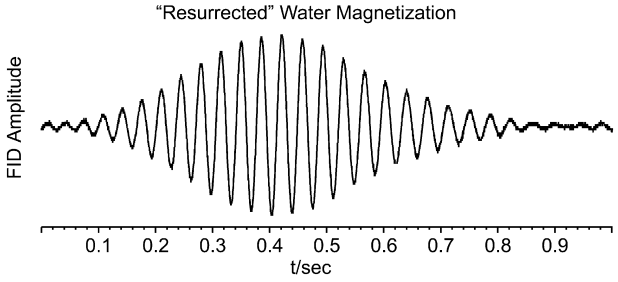

Fig. 7. Confirmation of "resurrected" transverse water magnetization after the application of a dephasing gradient to a 90%/10% H_2O/D_2O sample containing no solute and no relaxation agents. There is negligible magnetization immediately after the modest dephasing gradient ($G = 4\ Gcm^{-1}$ applied for 2 ms) has been applied to the magnetization from a 90° read pulse. However, a weak but significant water signal is observed at longer times, peaking around 500 ms after the termination of the gradients. While the residual signal is weak by comparison with the huge unsuppressed water signal, it is not insignificant compared to solute signals in the mM range.

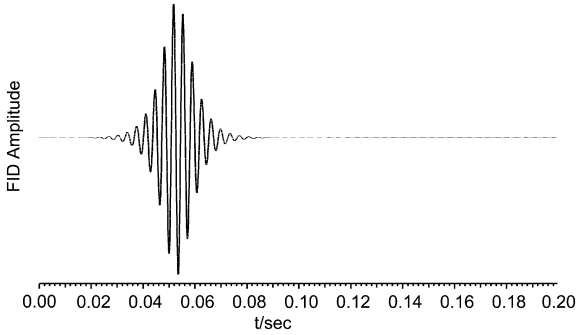

Fig. 8. Observation of radiation damping at 500 MHz with a conventional 5 mm H{CN} Varian triple resonance probe. The sample of Fig. 7 was used. A conventional 180° inversion pulse was followed with a 1 ms PFG of 15 Gcm^{-1}. The observed signal is enormous once it springs to life, necessitating the minimum receiver gain to capture it on scale. We observed this kind of FID when employing PFGs of 30 Gcm^{-1} and durations of 1–5 ms, indicating that the radiation damping is robust and not contingent on residual small amounts of transverse magnetization.

applied PFG, up to the strength and duration limits imposed by the hardware. The details of the water signal reemergence can depend on the presence or absence of other lines in the spectrum, apparently because the small currents in the RF coil stemming from the magnetization from these spins can destabilize the inverted water z-magnetization more or less quickly. Anomalous refocusing and spontaneous generation of transverse water magnetization from z-magnetization are mechanisms that both can lead to poor water suppression, and need to be kept in mind when manipulating z-magnetization. Saturating the H_2O resonance is usually not optimum for protein NMR in any event [3] making sequences like WET more the province of small-molecule applications.

4.2. Frequency profiles

Fig. 9 shows the experimental water suppression profile for the 3-9-19 WATERGATE sequence over a ±5 kHz

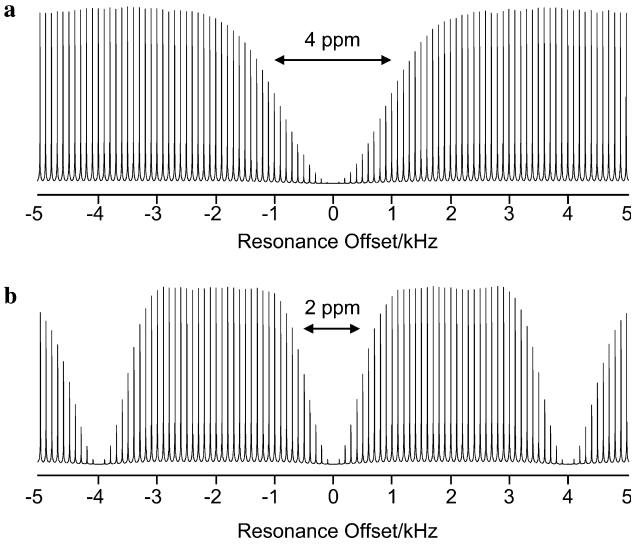

Fig. 9. Frequency profiles for the 3-9-19 hard-pulse WATERGATE sequence. A 10 μs 90° pulse ($\gamma B_1/2\pi = 25$ kHz) was applied near resonance, and then the transmitter frequency switched by the indicated amount before applying the WATERGATE pulse, at this same power level. The transmitter frequency was then restored to the original frequency and the FID recorded. Hopping the frequency is necessary to remove the offset dependence of the excitation pulse itself from the profile. (a) Interpulse delay $\tau = 125$ μs, showing good excitation bandwidth but a fairly broad area around the water line where signals would be attenuated. (b) Interpulse delay $\tau = 250$ μs, showing a narrower excitation bandwidth but a fairly narrow area around the water line where signals would be attenuated. As τ is the only adjustable parameter in the 3-9-19 WATERGATE method, the width of the notch is tied to the width of the passband.

range using either 125 or 250 μs delays. The periodic notch structure is illustrated in Fig. 9(b), which has a fairly narrow notch region, allowing signals close to the water peak to be observed, but which would be a drawback for the observation of protons far downfield, as may occur in RNA samples [29].

Fig. 10 shows the experimental water suppression profiles for soft-pulse WATERGATE [15], PURGE [19] and SOGGY. The WATERGATE and SOGGY profiles agree with the simulations of Fig. 2. The recently published PURGE sequence produces a more V-shaped profile that is somewhat disadvantageous in terms of the absolute suppression of the water line if the transmitter is offset slightly, and also with respect to the attenuation of lines near to water in frequency.

4.3. Small molecule water suppression

Fig. 11 shows an unbiased comparison of SOGGY with some of the other water suppression methods. No water flip-back pulse, which could have been used preceding the 90° read pulse, has been used here. These would be typical conditions for small molecule NMR, and allows the methods to be compared with the least complication.

The spectra of Fig. 11, all plotted on the same absolute scale and obtained under identical conditions, are from a standard 2 mM sucrose solution in 90%/10% H_2O/D_2O

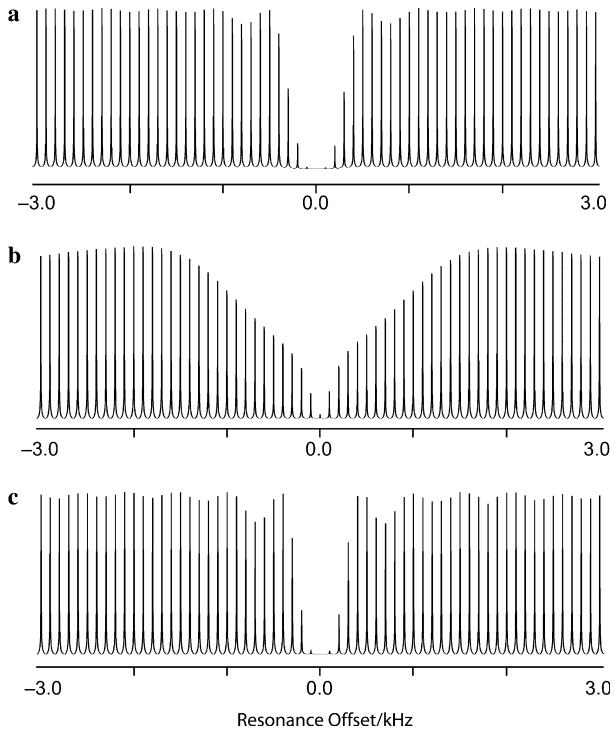

Fig. 10. Frequency profiles for some water suppression sequences, plotted over a narrower frequency range than Fig. 9, using the same RF power for the hard pulses. (a) Optimized soft-pulse WATERGATE, with 2 ms soft 90° pulses, $\gamma B_1/2\pi = 125$ Hz. The shape of the notch and extent of the undulations in amplitude agree well with the simulations of Fig. 2. The two PFGs were 1 ms in duration and 20 Gcm^{-1} in strength. (b) PURGE. A less useful profile emerges here because of the V-shaped notch, resulting in attenuation of resonances nearby the water. A 3 s presaturation pulse, $\gamma B_1/2\pi = 125$ Hz was applied, with the other parameters as specified in Ref. [19]. (c) SOGGY, using 2 ms soft 180° pulses, $\gamma B_1/2\pi = 250$ Hz, and the composite hard 180° pulse applied with $\gamma B_1/2\pi = 6.25$ kHz, corresponding to a 40 μs 90° pulse. The undulations are somewhat more pronounced than in WATERGATE, in accord with the simulations of spin–flip probability. The four PFGs were 500 μs in duration, the first pair at 20 Gcm^{-1} and the second at 6 Gcm^{-1}.

with 0.5 mM DSS and a trace of NaN_3 (CAT # DLM 7010, Cambridge Isotope Laboratories, Inc., Andover, Mass.). The points to note are (i) the absolute degree of suppression of the 90% H_2O peak; (ii) the intensity of the relatively nearby anomeric proton. An ancillary issue is the undesired *J*-modulation from proton scalar coupling that occurs with all spin echo methods. If both coupled spins are in the passband, then they are both flipped, and multiplets will appear with artificially enhanced splittings from the antiphase dispersive components. If, on the other hand, one coupling partner is in the notch region, then the coupling will rephase, although of course the lines in the notch region are suppressed along with the water.

4.4. Water suppression in protein NMR

Many proton-detected protein NMR sequences focus on the amide H_N resonances. These protons have pH-dependent chemical exchange with the water, so that saturation of the water resonance, even transiently, can reduce the observed sensitivity to a significant extent [3]. As sensitivity is often of primary importance, this issue should not be glossed over. Note that PURGE [19], which includes a presaturation of the water, should lead to loss of H_N signal intensity in protein NMR, through saturation transfer. The spectra of Ref. [19], Fig. 3 do not employ flip-back pulses for the WATERGATE sequences, and in this case the water is effectively saturated after the first transient. The net loss of H_N intensity will then depend on the relaxation delay between transients; for optimum sensitivity this is usually far shorter than the generous 3.0 s delay chosen in Ref. [19] and the loss will be greater. If no steady-state dummy scans are performed, the measured loss will also depend on how many transients are added to the first one. Temperature and pH are other relevant variables for exchanging protons. The comparison in Ref. [19] is thus somewhat misleading, because there is no NH region shown that is obtained under best current practice, particularly under conditions of fairly rapid pulsing, as would be usual in obtaining a 3D NMR spectrum.

Fig. 12 shows results obtained on a small, structured, well-behaved protein at pH 4.7, where the H_N exchange is not as rapid as at more physiological pH. By preceding the 90°(x) read pulse with a 5 ms 90°($-x$) selective pulse at the water frequency, the water magnetization was not saturated by the remainder of the SOGGY sequence. The water suppression was still excellent, so only the downfield region of the spectrum is shown. Predictably, the use of presaturation reduces the sensitivity of some of the signals, even with a generous 3.5 s delay between read pulses. As sensitivity is of paramount importance, it seems unlikely that presaturation will reemerge as a major factor in macromolecular NMR. Based on these results, the simulation profiles, applications to larger proteins (See Supplementary Material) and our overall experience with the method, we are confident in recommending SOGGY for general-purpose water suppression applications.

5. Conclusions

Solvent suppression remains an area of interest for NMR technique development, and the best compromise will be dictated by the details of the experiment, spectrometer hardware limitations, and other considerations such as the time it takes to optimize the performance on each sample, and the degree of suppression required. Many solvent suppression schemes have been proposed, and many of them are capable of excellent performance when adjusted by direct interactive observation of the residual solvent signal. But ease of use, generality, and robustness are important considerations for day-to-day general purpose use, particularly for water suppression. By replacing the conventional hard 180° pulse in the excitation sculpting motif proposed by Hwang and Shaka [16] with a simple phase-alternating composite pulse, compensation for B_1 inhomogeneity can be achieved over a reasonable range of resonance

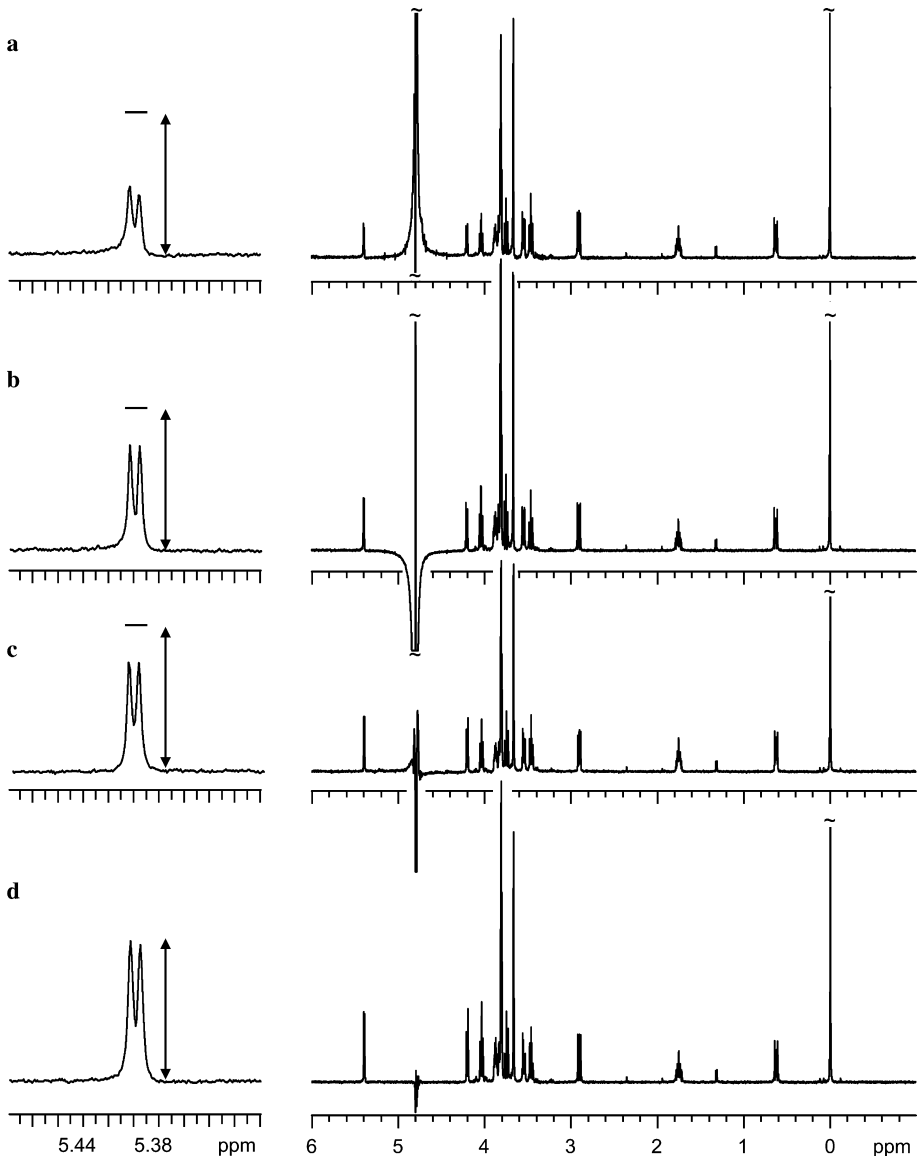

Fig. 11. Water suppression results on 2 mM sucrose in 90%/10% H_2O/D_2O. All spectra result from four transients, in which EXORCYCLE and CYCLOPS phase cycling were superimposed. Four steady-state transients preceded the acquisition of the data. The read pulse was always a 10 μs rectangular 90° pulse. The expansion panels on the left show the anomeric proton, with a vertical standard included to guide the eye. The full spectra are shown at the right. In some cases, where the water suppression is not high enough, or where the sharp TMS reference line is too strong, the peaks have been clipped with a symbol "~" to indicate this truncation. All spectra were taken sequentially, with the same spectrometer gain settings, shimming, *etc.* and when repeated several times on different occasions the results shown were fully reproducible. (a) 3-9-19 WATERGATE, $\tau = 333$ μs. A pair of 1 ms PFGs of 20 Gcm^{-1} with a stabilization delay of 150 μs was used to attenuate the water. There is noticeable attenuation of the anomeric doublet, and also attenuation of the TMS resonance as well. (b) Soft-pulse WATERGATE. PFGs and stabilization delays as in (a), and soft 90° pulses of 2 ms ($\gamma B_1/2\pi = 125$ Hz). (c) PURGE. The experimental details were taken from Ref. [19]. The presaturation time is 3 s with a weak field ($\gamma B_1/2\pi = 125$ Hz). (d) SOGGY. The width of the soft 180° pulses was 2 ms ($\gamma B_1/2\pi = 250$ Hz) and the composite 180° pulse was applied with $\gamma B_1/2\pi = 6.25$ kHz (40 μs 90° pulse width). The length of the composite 180° pulse was thus 296 μs. Each of the four PFGs was 500 μs, half the length of the WATERGATE PFGs, and the strengths were $G_1 = 20$ Gcm^{-1} and $G_2 = 6$ Gcm^{-1} with a stabilization delay of 150 μs. As such, the total gradient area is less for SOGGY than for WATERGATE, showing that the details of the pulse sequence matter for water suppression, and not simply the dephasing power of the PFGs. In these simple tests SOGGY gives the best water suppression, and also the best retention of the solute signals as measured by the anomeric doublet expansions.

offsets, so that good solute sensitivity can be realized while still achieving excellent suppression of the water line. The SOGGY sequence is only marginally more complex than the existing DPFGSE sequence, and works well in both small and large molecule applications. By scaling the duration of only the composite pulse sequence, very large bandwidths can be obtained, allowing trouble-free observation of signals far down- or up-field without the limitations of 3-9-19 WATERGATE. Scaling the entire SOGGY sequence inversely to the spectrometer frequency allows simple translation between different magnetic field strengths, giving optimum sensitivity and excellent water suppression. Unlike PURGE, SOGGY can be incorporated in water flip-back experiments, in cases where chemical

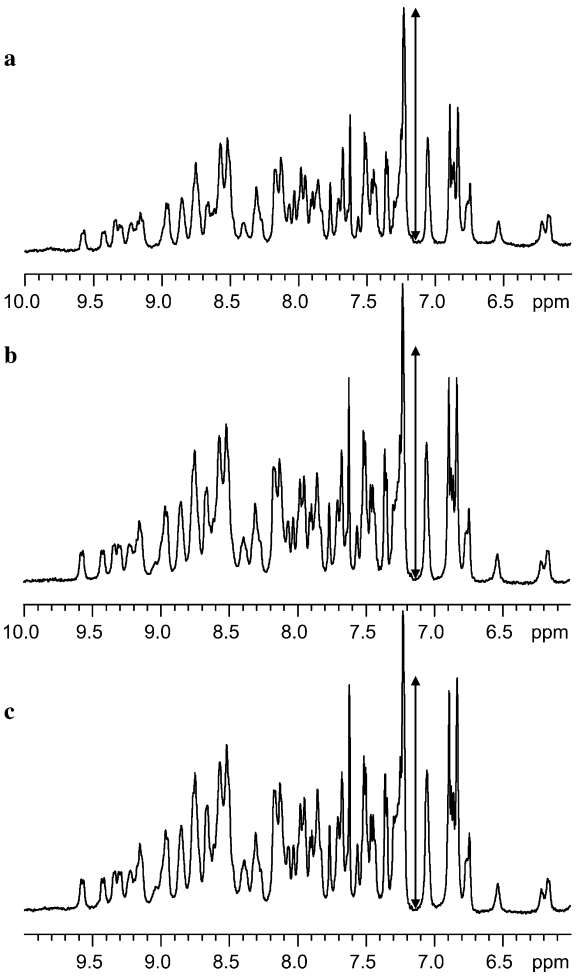

Fig. 12. A comparison of three water suppression methods applied to a protein under conditions where amide exchange is predicted to be fairly slow. The protein sample was a 1 mM sample of human ubiquitin at pH 4.7, 2.5 mM acetate buffer, in 90%/10% H_2O/D_2O and 25 °C. Four transients were acquired for each spectrum and the time between scans (acquisition time plus additional delay) was 3.5 s. (a) PURGE, using conditions from Ref. [19], a 62.5 Hz (−6 dB versus the data in Fig. 11) presaturation RF field for 3 s. (b) SOGGY, using the same parameters as in Fig. 11 and (c) SOGGY with a water flipback pulse of 5 ms duration preceding the sequence in (b). As in Fig. 11, four steady-state transients preceded the data acquisition. The double-arrow vertical standard matches the intensity of the resonance at 7.23 ppm in the PURGE spectrum. The other two spectra show markedly better sensitivity for this peak. Some of the H_N peaks are almost a factor of two larger, while others show more modest gains. With faster pulsing (1 Hz repetition rate) the losses with PURGE were substantially greater and the water suppression suffered somewhat.

exchange would otherwise reduce sensitivity [3]. As such, SOGGY seems to have a number of important advantages compared with the existing state of the art.

Acknowledgments

This research was made possible by support from the National Institutes of Health, GM- 66763, and by a UC Discovery Grant BIO05-10533. K.J.D. was supported by the National Institutes of Health, National Research Service Award 5 T15 LM007443 from the National Library of Medicine. B.D.N. thanks the UCI School of Physical Sciences for partial support.

Appendix A. Supplementary data

Supplementary data associated with this article can be found, in the online version, at doi:10.1016/j.jmr.2006.10.014.

References

[1] J. Schaefer, Selective saturation of C-13 lines in C-13 Fourier-transform NMR experiments, J. Magn. Reson. 6 (1972) 670–671.
[2] D.I. Hoult, Solvent peak saturation with single-phase and quadrature Fourier transformation, J. Magn. Reson. 21 (1976) 337–347.
[3] S. Grzesiek, A. Bax, The importance of not saturating H_2O in protein NMR. Application to sensitivity enhancement and NOE measurements, J. Am. Chem. Soc. 115 (1993) 12593–12594.
[4] R.A. Hoffman, S. Forsen, B. Gestblom, Method for analysis of high-resolution NMR spectra employing transitory selective saturation, J. Chem. Phys. 39 (1963) 486–487.
[5] S.L. Patt, B.D. Sykes, Water eliminated Fourier-transform NMR spectroscopy, J. Chem. Phys. 56 (1972) 3182–3184.
[6] R.K. Gupta, Dynamic range problem in Fourier-transform NMR. Modified WEFT pulse sequence, J. Magn. Reson. 24 (1976) 461–465.
[7] A.G. Redfield, R.K. Gupta, Pulsed Fourier-transform NMR spectrometer for use with H_2O solutions, J. Chem. Phys. 54 (1971) 1418–1419.
[8] P. Plateau, M. Gueron, Exchangeable proton NMR without baseline distortion, using new strong-pulse sequences, J. Am. Chem. Soc. 104 (1982) 7310–7311.
[9] A.G. Redfield, S.D. Kunz, E.K. Ralph, Dynamic range in Fourier-transform proton magnetic resonance, J. Magn. Reson. 19 (1975) 114–117.
[10] D.L. Turner, Binomial solvent suppression, J. Magn. Reson. 54 (1983) 146–148.
[11] P.J. Hore, A new method for water suppression in the proton NMR spectra of aqueous solutions, J. Magn. Reson. 54 (1983) 539–542.
[12] P.J. Hore, Solvent suppression in Fourier-transform nuclear magnetic resonance, J. Magn. Reson. 55 (1983) 283–300.
[13] R.E. Hurd, Gradient-enhanced spectroscopy, J. Magn. Reson. 87 (1990) 422–428.
[14] M. Piotto, V. Saudek, V. Sklenar, Gradient-tailored excitation for single-quantum NMR spectroscopy of aqueous solutions, J. Biomol. NMR 2 (1992) 661–665.
[15] V. Sklenar, M. Piotto, R. Leppik, V. Saudek, Gradient-tailored water suppression for ^1H-^{15}N HSQC experiments optimized to retain full sensitivity, J. Magn. Reson. Ser. A 102 (1993) 241–245.
[16] T.L. Hwang, A.J. Shaka, Water suppression that works. Excitation sculpting using arbitrary waveforms and pulsed field gradients, J. Magn. Reson. Ser. A 112 (1995) 275–279.
[17] S.H. Smallcombe, S.L. Patt, P.A. Keifer, WET solvent suppression and its applications to LC NMR and high-resolution NMR spectroscopy, J. Magn. Reson. Ser. A 117 (1995) 295–303.
[18] M.L. Liu, X.A. Mao, C.H. Ye, H. Huang, J.K. Nicholson, J.C. Lindon, Improved WATERGATE pulse sequences for solvent suppression in NMR spectroscopy, J. Magn. Reson. 132 (1998) 125–129.
[19] A.J. Simpson, S.A. Brown, Purge NMR: Effective and easy solvent suppression, J. Magn. Reson. 175 (2005) 340–346.
[20] K. Stott, J. Stonehouse, J. Keeler, T.L. Hwang, A.J. Shaka, Excitation sculpting in high-resolution NMR spectroscopy: Application to selective NOE experiments, J. Am. Chem. Soc. 117 (1995) 4199–4200.

[21] N. Bloembergen, R.V. Pound, Radiation damping in magnetic resonance experiments, Phys. Rev. 95 (1954) 8–12.
[22] M.P. Augustine, Transient properties of radiation damping, Prog. NMR Spectrosc. 40 (2001) 111–150.
[23] Y.-Y. Lin, N. Lisitza, S. Ahn, W.S. Warren, Resurrection of crushed magnetization and chaotic dynamics in solution NMR spectroscopy, Science 290 (2000) 118–121.
[24] G.A. Morris, R. Freeman, Selective excitation in Fourier transform nuclear magnetic resonance, J. Magn. Reson. 29 (1978) 433–462.
[25] M.A. Smith, H. Hu, A.J. Shaka, Improved broadband inversion performance for NMR in liquids, J. Magn. Reson. 151 (2001) 269–283.
[26] A.J. Shaka, Composite pulses for ultra-broadband inversion, Chem. Phys. Lett. 120 (1985) 201–205.
[27] A.J. Shaka, J. Keeler, T. Frenkiel, R. Freeman, An improved sequence for broadband decoupling: WALTZ-16, J. Magn. Reson. 52 (1983) 335–338.
[28] A.J. Shaka, J. Keeler, R. Freeman, Evaluation of a new broadband decoupling sequence: WALTZ-16, J. Magn. Reson. 53 (1983) 313–340.
[29] M.P. Latham, D.J. Borwn, S.A. McCallum, A. Pardi, NMR methods for studying the structure and dynamics of RNA, Chembiochem. 6 (2005) 1492–1505.